To appear in AIAA GNC 2011

Distributed Estimation for Motion Coordination in an Unknown Spatiotemporal Flowfield

Cameron K. Peterson* and Derek A. Paley†

University of Maryland, College Park, MD, 20742, USA

Cooperating autonomous vehicles perform better than uncooperating vehicles for applications such as surveillance, environmental sampling and target tracking. For multiple vehicles to cooperate effectively, the navigation control laws should account for disturbances caused by ocean currents or atmospheric winds. This paper provides dynamic decentralized control algorithms for motion coordination in an unknown, time-invariant flowfield. The algorithms simultaneously estimate the flowfield and use that estimate in an observer-based feedback control that stabilizes a moving formation. Each vehicle uses noisy measurements of its own position to generate independent flowfield estimates. For a uniform flowfield, we provide a theoretically justified approach for each vehicle to estimate the flow independently. For a nonuniform flowfield, we propose a distributed algorithm using an information filter to reconstruct the flowfield and a consensus filter to share information between vehicles. In either case, the vehicles use the flowfield estimate to steer to a circular formation.

Nomenclature

a_n Flowfield coefficient, $n = 1, \ldots, l$

c_k Center of circle traversed by particle k

C_k Covariance matrix for particle k

$e_{1,k}$ Position error for particle k, $e_{1,k} \in \mathbb{R}$

*Graduate student, Department of Aerospace Engineering; cammykai@yahoo.com. AIAA Student Member.

†Assistant Professor, Department of Aerospace Engineering; dpaley@umd.edu. AIAA Associate Fellow.

$e_{2,k}$ Flowfield error for particle k, $e_{2,k} \in \mathbb{R}$

$\boldsymbol{e}_{3,k}$ Coefficient error matrix for particle k, $e_{3,k} \in \mathbb{R}^{l\times 1}$

f_k Flow velocity at position r_k

$g_k(t)$ Bounded state perturbation for particle k at time t

I_k Information matrix for particle k

K Kalman filter gain matrix

K_m Control algorithm gains, $m = 1, \ldots, 3$

K_P Consensus filter proportional gain

K_I Consensus filter integral gain

m_k Measured position difference for particle k

M Error covariance matrix

N Number of particles

P $N \times N$ projector matrix

P_k kth row of matrix P

r_k Position of particle k

$\dot{r}_k$ Inertial velocity of particle k

R_k Measurement variance of particle k, $R \in \mathbb{R}$

s_k Inertial speed of particle k at time t

u_k flow-relative steering control of particle k

v_k Measurement noise for particle k

$\boldsymbol{y}_k$ Measurement matrix for particle k, $\boldsymbol{y} \in \mathbb{R}^{l\times 1}$

γ_k Orientation of the inertial velocity of particle k

δ Perturbation bound

η_k Consensus filter integrator term for particle k

ν_k Steering control of particle k

ω_0 Constant angular rate

ϕ Consensus filter gain factor, $\phi \in \mathbb{R}$

$\boldsymbol{\psi}_k$ Flowfield basis vector evaluated at the position of particle k, $\boldsymbol{\psi}_k \in \mathbb{R}^{l\times 1}$

τ_k Consensus variable for particle k

θ_k Orientation of the flow-relative velocity of particle k

Subscript and Superscripts

k Particle indices, $k = 1, \ldots, N$

I. Introduction

Cooperation between vehicles improves performance for multi-vehicle tasks such as environmental sampling, target identification, tracking, and surveillance. Recent research has focused on designing cooperative-control algorithms to perform these tasks autonomously.[1–6] Unknown flowfields such as winds or currents disrupt the motion of an autonomous vehicle in the atmosphere or ocean. These disturbances are difficult to model and may contribute to a significant portion of the vehicle's inertial velocity. Ensuring vehicles work together in the presence of a temporally and spatially varying flowfield is an ongoing challenge that is partially addressed in this paper. Cooperative-control algorithms are provided for multiple autonomous vehicles in the presence of an unknown spatially varying flowfield. We limit the flowfields to be of moderate intensity, i.e., the flowfield does not exceed the vehicle's speed relative to the flow.

Some existing algorithms support operation in an unknown, spatially uniform flow. Summers et al. account for a constant-velocity wind using adaptive estimates to drive cooperative vehicles in a loiter circle.[2] Burger and Pettersen enable curved trajectory following of surface vehicles by using a conditional integrator to eliminate constant disturbances for vehicle formations.[6] Peterson and Paley use knowledge of the vehicle's position to dynamically stabilize multiple vehicles to a circular formation in a spatially uniform flowfield.[7] All these approaches require that the estimation value be spatially invariant.

Estimation of spatially varying environmental fields, such as temperature, was performed by Lynch et al. using multiple vehicles and a decentralized PI consensus filter.[8] Consensus filters provide an effective way to achieve distributed control of many vehicles with communication constraints.[9,10] The scalar field estimate was coupled with a gradient control to move the vehicles into sampling positions that minimized the uncertainty. For constant, connected communication between stationary particles, using a consensus filter ensures convergence to the average of all the consensus inputs. The decentralized filter converges to the same result as a centralized filter.[8]

A consensus filter was also used in combination with an information filter by Casbeer and Beard to estimate the state of a system.[11,12] Their work shows that when the consensus filter did not converge prior to estimating the state, the decentralized error covariance estimates were overly conservative, but the estimated state was close to the one obtained with the centralized estimator. Olfati-Saber has also worked extensively with decentralized Kalman filter approaches.[13–16] He developed techniques applicable to a heterogeneous group of sensors[13] and proved stability for the information-consensus filter.[16]

The work we present also adopts a distributed information-consensus filter to estimate the coefficients of a parameterized flowfield, assuming knowledge of a set of basis vectors common to all vehicles. The inter-vehicle communication constraints may be time-varying, provided they are strongly connected over time.[10] The estimated flowfield and its directional derivative at the vehicle locations are fed into decentralized control laws that cooperatively stabilize vehicles to circular formations. We model each autonomous vehicle as a Newtonian point mass particle[3,17] that has a steering control perpendicular to the velocity relative to the flowfield and travels at constant, unit speed relative to the flow. We initially assume each vehicle measures the local flowfield at its current position. We later relax this assumption and require only noisy position measurements to approximate the local flowfield. Spatially varying flowfields are estimated using a centralized information filter when all-to-all communication is available, and a consensus filter when limited communication exists.

This paper extends the authors' previous work[7] on estimating spatially invariant flowfields using perfect position measurements. We provide an algorithm for a spatially variable flowfield and prove robustness to measurement noise. We also show that by sharing measurements between vehicles, we can improve performance in a spatially-varying flowfield. The contributions of this paper are (1) the stabilization of circular formations in an estimated, uniform flow using only noisy position measurements, and (2) the stabilization of circular formations in a estimated spatially varying flowfield using a decentralized information-consensus filter with noisy position measurements.

The paper proceeds as follows. Section II introduces the vehicle model and summarizes previous work on motion coordination in an estimated spatially uniform flowfield. It also outlines the algorithm for decentralized estimation of a scalar field. Section III shows that the estimator presented in Section II is robust to measurement noise. Section IV introduces control algorithms that stabilize circular formations in an unknown spatially varying flowfield using an information-consensus filter. Conclusions and highlights of ongoing work are given in Section V.

II. Background: Motion Coordination and Distributed Estimation of a Scalar Field

This section introduces the vehicle model and summarizes previous results for the simultaneous estimation of a flowfield and use of that estimate in a multi-vehicle control. Section II.A describes a formation control algorithm that drives multiple vehicles to a circular formation in an unknown flowfield. The flowfield is estimated individually by each vehicle using noise free position measurements. Sharing estimates between vehicles enables multi-vehicle formations in unknown spatially varying flowfield. Section II.B summarizes prior results for the estimation of a scalar field using a distributed algorithm. Specifically, we summarize the information filter[18] and a PI consensus filter.[8]

A. Multi-Vehicle Motion Coordination in an Unknown Flowfield

In this paper, each autonomous vehicle is modeled as a self-propelled Newtonian particle. The particle travels at constant, unit speed relative to an ambient flowfield (e.g., wind or ocean currents). It is subject to a steering control that acts perpendicular to the velocity of the vehicle relative to the flowfield. In general the flowfield $f_k = f(t, r_k)$ may be spatially and temporally varying. We assume that the flowfield does not exceed the speed of a particle, i.e., $|f_k| < 1$, which guarantees the particle can always exhibit forward motion in the inertial (ground-fixed) frame. The position of a single particle, indexed by $k = 1, \ldots, N$, is denoted by r_k. The particle's inertial velocity is $\dot{r}_k$ and the equations of motion are

$$\begin{aligned} \dot{r}_k &= e^{i\theta_k} + f_k \\ \dot{\theta}_k &= u_k. \end{aligned} \tag{1}$$

The steering control u_k is the turn rate of the orientation θ_k of the velocity relative to the flow. Generally an autonomous vehicle will have physical constraints limiting its turning rate. However, in this paper we ignore these constraints because we have shown elsewhere[7] that they do not impact the main theoretical results for multi-vehicle coordination. Rewriting the equations of motion in terms of an inertial speed and orientation gives

$$\begin{aligned} \dot{r}_k &= s_k e^{i\gamma_k} \\ \dot{\gamma}_k &= \nu_k, \end{aligned} \tag{2}$$

where $\gamma_k = \arg(\dot{r}_k)$ is the orientation of the inertial velocity of the kth particle and $s_k = s(t, r_k, \theta_k) = |\dot{r}_k|$ denotes its magnitude. ν_k is the angular rate of change of the inertial-velocity orientation of particle k. We use Lyapunov-based control to design ν_k; the vehicle control u_k is recoverable from ν_k as long as $|f_k(t)| < 1$.[17]

In the presence of a constant flowfield whose direction may be rotating in time, a dynamic control with a flowfield estimator can be used to stabilize a circular formation. The estimated flowfield is $\hat{f}_k = \hat{f}(t, r_k)$. Assume that particle k knows its position r_k and velocity orientation θ_k. The estimated inertial velocity and dynamics are

$$\begin{aligned} \dot{\hat{r}}_k &= \hat{s}_k e^{i\hat{\gamma}_k} \\ \dot{\hat{\gamma}}_k &= \nu_k, \end{aligned} \tag{3}$$

where $\hat{s}_k$ and $\hat{\gamma}_k$ are the magnitude and orientation, respectively, of the estimated inertial velocity for particle k. The control algorithm works by dynamically estimating the flowfield and then using that estimate to steer the particles as described next.

Let the estimation error for particle k be $e_{1,k} = \hat{r}_k - r_k$ and $e_{2,k} = \hat{f}_k - f_k$. Consider the estimator dynamics[7]

$$\begin{aligned} \dot{\hat{r}}_k &= e^{i\theta_k} + \hat{f}_k - K_1(\hat{r}_k - r_k) \\ \dot{\hat{f}}_k &= -K_2(\hat{r}_k - r_k). \end{aligned} \tag{4}$$

In matrix form, the estimation-error dynamics for particle k are

$$\begin{bmatrix} \dot{e}_{1,k} \\ \dot{e}_{2,k} \end{bmatrix} = \begin{bmatrix} -K_1 & 1 \\ -K_2 & 0 \end{bmatrix} \begin{bmatrix} e_{1,k} \\ e_{2,k} \end{bmatrix}. \tag{5}$$

Choosing gains $K_2 > 0$ and $K_1 = 2\sqrt{K_2} > 0$ exponentially stabilizes the origin $e_{1,k} = e_{2,k} = 0\,\forall\, k$.[7]

Next we describe a control law to stabilize a set of particles to a circular formation centered at $\hat{c}_k$ where[7]

$$\hat{c}_k = \hat{r}_k + \omega_0^{-1} i e^{i\hat{\gamma}_k}. \tag{6}$$

Differentiating (6) we find a steering control ν_k for which $\dot{\hat{c}}_k = 0$. This control law ensures that the estimated circle center is fixed and particle k will travel at a constant radius around this center point. We have

$$\dot{\hat{c}}_k = \hat{s}_k e^{i\hat{\gamma}_k} - \omega_0^{-1} e^{i\hat{\gamma}_k} \nu_k = (\hat{s}_k - \omega_0^{-1}\nu_k) e^{i\hat{\gamma}_k}. \tag{7}$$

Control $\nu_k = \omega_0 \hat{s}_k$ allows us to drive a single particle around a circle with radius $|\omega_0|^{-1}$ at the estimated center point.

Consider the Lyapunov function

$$\hat{S}(\hat{\boldsymbol{r}}, \hat{\boldsymbol{\gamma}}) \triangleq \frac{1}{2}\langle \hat{\mathbf{c}}, P\hat{\mathbf{c}} \rangle + \frac{1}{2}\left(||\boldsymbol{e}_1||^2 + ||\boldsymbol{e}_2||^2 \right), \tag{8}$$

where $\boldsymbol{e}_1 = [e_{1,1}, e_{1,2}, ..., e_{1,N}]^T$ and $\boldsymbol{e}_2 = [e_{2,1}, e_{2,2}, ..., e_{2,N}]^T$. Let $\mathbf{1} = [1, \ldots, 1]^T \in \mathbb{R}^N$. P is the $N \times N$ projection matrix

$$P = \text{diag}\{\mathbf{1}\} - \frac{1}{N}\mathbf{1}\mathbf{1}^T, \tag{9}$$

which is equivalent to the Laplacian matrix of an all-to-all communication topology.[19] $\hat{S}$ is equal to zero when $\hat{\mathbf{c}} = c_0\mathbf{1}$, $c_0 \in \mathbb{C}$, and the estimation errors are zero.

We have the following result [7, Theorem 4].

Theorem 1. *Let $f_k = \beta(t) \in \mathbb{R}$ satisfy $|\beta| < 1$. Also, let $\hat{r}_k$ and $\hat{f}_k$ evolve according to (4) with $K_2 > 0$ and $K_1 = 2\sqrt{K_2}$. Choosing the control*

$$\nu_k(t) = \omega_0(\hat{s}_k + K_3\langle P_k\hat{\mathbf{c}}, e^{i\hat{\gamma}_k}\rangle),\; K_3 > 0, \tag{10}$$

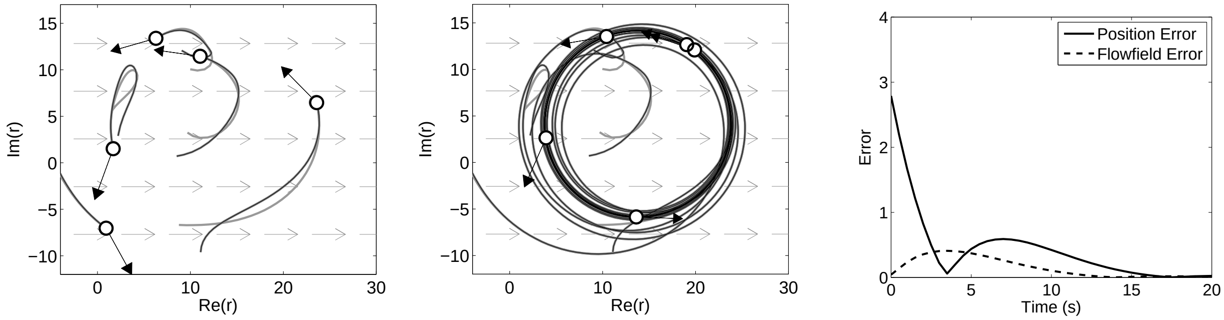

(a) Uniform flow, $t = 20$ s (b) Uniform flow, $t = 500$ s (c) Particle $k = 3$ Error Dynamics

Figure 1. Stabilization of circular formation in an unknown uniform flowfield $f = 0.6$.

forces convergence of solutions of model (3) to the set of a circular formations with radius $|\omega_0|^{-1}$ and direction determined by the sign of ω_0.

Theorem 1 is proven by showing that the control (10) makes $\dot{\hat{S}} \leq 0$. The set $\{\dot{\hat{S}} = 0\}$ is achieved only when $\nu_k = \omega_0 \hat{s}_k$ for all k, which is our criteria for a circular configuration. In order to use ν_k to solve for the turn-rate control u_k (which is the input to the vehicle model (1)) we need the flowfield $f_k(t)$ and the directional derivative $\dot{f}_k(t)$ of the flowfield,[7] given by $\dot{f}_k = (\partial f_k / \partial r_k)\, \dot{r}_k + \frac{\partial f_k}{\partial t}$.

Figure 1 illustrates simulation results for model (3) and control (10) with estimator gains $K_2 = 0.2$ and $K_1 = 2\sqrt{K_2} = 0.894$. The magnitude of the spatially uniform flowfield is 0.6. Figures 1(a) and 1(b) show tracks of the estimated (darker track) and actual (lighter track) particle positions at 20 and 500 seconds respectively. After 20 seconds the particles have estimated the flowfield and eliminated the flowfield and position error. After 500 seconds the particles have also converged to a circular configuration. Figure 1(c) displays the error between the actual and estimated position, $\hat{r}_k - r_k$, and flowfield, $\hat{f}_k - f_k$, for particle $k = 3$.

B. Multi-Vehicle Estimation of an Unknown Scalar Field

This section summarizes the work of Lynch et al.[8] in which an information filter and a PI consensus filter were used to estimate an environmental scalar field using measurements collected by multiple vehicles. In Section IV we use the same process to estimate a vector flowfield. Let the environmental field be approximated at position r_k with a set of l basis vectors[8]

$$f_k = \sum_{n=1}^{l} a_n \psi_n(r_k), \tag{11}$$

where $\boldsymbol{\psi}(r_k) \triangleq \boldsymbol{\psi}_k = [\psi_1(r_k), \psi_2(r_k), ..., \psi_l(r_k)]^T$ are the basis vectors evaluated at r_k and $\boldsymbol{a} = [a_1, a_2, ..., a_l]^T$ are the flowfield coefficients. The coefficients must be estimated in order to recover the field, but it is assumed that the basis vectors are known.

The measurement for each vehicle is[8]

$$\tilde{f}_k = \boldsymbol{\psi}_k^T \boldsymbol{a} + v_k \tag{12}$$

where v_k is Gaussian, zero-mean measurement noise with variance $R_k \in \mathbb{R}$. Although Lynch et al. allow the coefficients to be time-varying, here we assume that the coefficients are constant, i.e. $\dot{a}_n = 0$ for all n, and estimate them using an information filter.

The information filter is a variation of the Kalman filter that propagates forward the inverse of the estimate uncertainty covariance. Let $M = E[(\boldsymbol{a}-\hat{\boldsymbol{a}})(\boldsymbol{a}-\hat{\boldsymbol{a}})^T]$ be the coefficient error covariance.[a] The inverse error covariance $I \triangleq M^{-1}$ is the information matrix. Note that infinite uncertainty in the estimated state results when I approaches zero or I has no state information. Knowing the state exactly gives infinite information and $I \to \infty$.[18] The information measurement is $\boldsymbol{i} = I\boldsymbol{a}$.[8] Using an information filter instead of a standard Kalman filter simplifies the amount of data that must be shared between vehicles since the update information is encompassed in a single covariance matrix and measurement vector.[12]

The information filter equations are obtained by substituting $M = I^{-1}$ and $\hat{\boldsymbol{a}} = I^{-1}\hat{\boldsymbol{i}}$ into the standard Kalman filter equations. For this work we implemented a discrete form of the information filter. Let t be the current time and Δt indicate a single time step. Also, let the superscript $^{(-)}$ equal the prior estimates and $^{(+)}$ indicate the updated estimate equations. The information filter equations are simplified under the assumption that the state $\boldsymbol{a}$ is constant and does not have process noise. These conditions imply that the predicted information covariance and information state at time t are equal to the prior values, i.e. $I^-(t) = I^+(t-\Delta t)$ and $\hat{\boldsymbol{i}}^-(t) = \hat{\boldsymbol{i}}^+(t-\Delta t)$. For particle k the measurement-update equations are[8,18]

$$\begin{aligned} I_k^+(t) &= I_k^-(t) + \boldsymbol{\psi}_k R_k^{-1} \boldsymbol{\psi}_k^T \\ \hat{\boldsymbol{i}}_k^+(t) &= \hat{\boldsymbol{i}}_k^-(t) + \boldsymbol{\psi}_k R_k^{-1} \tilde{f}_k. \end{aligned} \tag{13}$$

Rewriting these equations using $C_k \triangleq \boldsymbol{\psi}_k R_k^{-1} \boldsymbol{\psi}_k^T$ and $\boldsymbol{y}_k \triangleq \boldsymbol{\psi}_k R_k^{-1} \tilde{f}_k$ yields[8]

$$\begin{aligned} I_k^+(t) &= I_k^-(t) + C_k \\ \hat{\boldsymbol{i}}_k^+(t) &= \hat{\boldsymbol{i}}_k^-(t) + \boldsymbol{y}_k. \end{aligned} \tag{14}$$

The matrix C_k and vector $\boldsymbol{y}_k$ represent the information gained from particle k in a single update measurement. The coefficients $\hat{\boldsymbol{a}}_k$ estimated by particle k can be obtained from the information matrix using[8] $\hat{\boldsymbol{a}}_k = I_k^{-1}\hat{\boldsymbol{i}}_k$. An advantage of using the information filter is that measurement updates are simply added to the predicted information covariance and vector.

[a] $E[(\cdot)]$ is the expected value of $(\cdot)$.

Multiple measurements may be incorporated in a single update step using the summation[8]

$$C \triangleq \sum_{k=1}^{N} C_k = \sum_{k=1}^{N} \boldsymbol{\psi}_k R_k^{-1} \boldsymbol{\psi}_k^T \tag{15}$$

and

$$\boldsymbol{y} \triangleq \sum_{k=1}^{N} \boldsymbol{y}_k = \sum_{k=1}^{N} \boldsymbol{\psi}_k R_k^{-1} \tilde{f}_k. \tag{16}$$

The measurement-update equations that incorporate the information from all particles are

$$\begin{aligned} I^+(t) &= I^-(t) + C \\ \hat{\boldsymbol{i}}^+(t) &= \hat{\boldsymbol{i}}^-(t) + \boldsymbol{y}, \end{aligned} \tag{17}$$

with the estimated coefficients $\hat{\boldsymbol{a}} = I^{-1}\hat{\boldsymbol{i}}$.

Notice that the measurement variance R_k is wrapped into the information update of C_k and $\boldsymbol{y}_k$, making it easier to share information among heterogeneous sensors groups since all the information is encapsulated in those two matrices. Let $C_{(i,j),k}$ indicate the entry in the ith row and jth column of C_k. Likewise $y_{n,k}$ is the nth entry of vehicle k's measurement vector.

A centralized information filter can be used directly to estimate $\hat{\boldsymbol{a}}$ when all-to-all communication is available. When all-to-all communication is unavailable, the information filter is supplemented by a consensus filter. The consensus filter approximates the average value of a given input parameter and converges to the true average as long as the vehicle communication topology is strongly connected over time.[10] We use the information-consensus filter to allow each vehicle to approximate C and $\boldsymbol{y}$ using only information from particles in that vehicle's neighbor set $\mathcal{N}_k$. The PI consensus filter is[8]

$$\begin{aligned} \dot{\tau}_k &= \phi(\tau_{0,k} - \tau_k) - K_P \textstyle\sum_{j\in\mathcal{N}_k}(\tau_k - \tau_j) + K_I \textstyle\sum_{j\in\mathcal{N}_k}(\eta_k - \eta_j) \\ \dot{\eta}_k &= -K_I \textstyle\sum_{j\in\mathcal{N}_k}(\tau_k - \tau_j) \end{aligned} \tag{18}$$

where $\tau_{0,k}$ is particle k's input to the estimated value, e.g. $\tau_{0,k} = C_{(i,j),k}$ where $i, j = [1, \ldots, l]$ or $y_{n,k}$ where $n = 1, \ldots, l$. $\phi \in \mathbb{R}$ is a gain factor determining how reliant the consensus filter is upon its own input. τ_k is the consensus value, i.e., the approximate average of $C_{(i,j),k}$ or $y_{n,k}$. η_k is an integrator term that is only used within the filter equations (18). K_P and K_I are the proportional and integral gains, respectively. The sums are computed for all the particles in the neighbor set of k, where $j \in \mathcal{N}_k$ indicates that vehicle k receives communication from vehicle j.

III. Flowfield Estimation Using Noisy Position Measurements

In this section we show that the observer based control law from Section II.A stabilizes particles to a circular formation even with imperfect measurements of particle positions. We assume a uniform flowfield and use the estimator introduced in Section II. In Section IV, we extend this result to spatially varying flowfields.

Let the position measurement be

$$\tilde{r}_k = r_k + g_k(t), \tag{19}$$

where $g_k(t)$ is bounded noise such as from GPS error or underwater navigation error. The error dynamics (4) become

$$\begin{aligned} \dot{\hat{r}}_k &= e^{i\theta_k} + \hat{f}_k - K_1(\hat{r}_k + g_k(t) - r_k) \\ \dot{\hat{f}}_k &= -K_2(\hat{r}_k + g_k(t) - r_k). \end{aligned} \tag{20}$$

In matrix form the estimator-error dynamics represent a perturbed system:

$$\begin{bmatrix} \dot{e}_{1,k} \\ \dot{e}_{2,k} \end{bmatrix} = \underbrace{\begin{bmatrix} -K_1 & 1 \\ -K_2 & 0 \end{bmatrix}}_{\triangleq B} \begin{bmatrix} e_{1,k} \\ e_{2,k} \end{bmatrix} - g_k(t) \begin{bmatrix} K_1 \\ K_2 \end{bmatrix}. \tag{21}$$

Choosing $Q \in \mathbb{R}^{2\times 2}$ to be the identity matrix, the solution to the Lyapunov equation $PB + B^T P = -Q$ is

$$P = \begin{bmatrix} \frac{(K_2+1)}{2K_1} & -\frac{1}{2} \\ -\frac{1}{2} & \frac{(K_2+K_1^2+1)}{2K_1K_2} \end{bmatrix}. \tag{22}$$

Let $c_1 = \lambda_{min}(P)$, $c_2 = \lambda_{max}(P)$, $c_3 = -\lambda_{min}(Q) = 1$, and $c_4 = 2\lambda_{max}(P)$, where λ represents the matrix eigenvalue. Also let $\boldsymbol{e}_k = [e_{1,k}, e_{2,k}]^T$.

Lemma 1. *Given the perturbed system (21) and bounded perturbations*

$$|g_k(t)\max(K_1, K_2)| \leq \delta < \frac{c_3}{c_4}\sqrt{\frac{c_1}{c_2}}x\epsilon \tag{23}$$

with $0 < \epsilon < 1$ *and* $||\boldsymbol{e}_k(t)|| < x$*. For all* $||\boldsymbol{e}_k(t_0)|| < \sqrt{\frac{c_1}{c_2}}x$ *the solution to the perturbed system (21) will obey*

$$\|\boldsymbol{e}_k(t)\| \leq \sqrt{\frac{c_2}{c_1}} e^{\xi(t-t_0)} \|e(t_0)\|,$$

where

$$\xi = \frac{(1-\epsilon)c_3}{2c_2} \tag{24}$$

and $\|\boldsymbol{e}_k(t)\|$ *is ultimately bounded by*

$$\|\boldsymbol{e}_k(t)\| \leq \frac{c_4}{c_3}\sqrt{\frac{c_2}{c_1}\frac{\delta}{\epsilon}}. \tag{25}$$

Proof. With candidate Lyapunov function $V(\boldsymbol{e}_k) = \boldsymbol{e}_k^T P \boldsymbol{e}_k$, the unperturbed system satisfies

$$\begin{aligned}
c_1\|\boldsymbol{e}_k(t)\|^2 &\leq V(\boldsymbol{e}_k) \leq c_2\|\boldsymbol{e}_k(t)\|^2 \\
\frac{\partial V}{\partial \boldsymbol{e}_k} &\leq -c_3\|\boldsymbol{e}_k(t)\|^2 \\
\left\|\frac{\partial V}{\partial \boldsymbol{e}_k}\right\|^2 &\leq c_4\|\boldsymbol{e}_k(t)\|^2.
\end{aligned}$$

where $c_1 = \lambda_{min}(P)$, $c_2 = \lambda_{max}(P)$, $c_3 = -\lambda_{min}(Q) = 1$, and $c_4 = 2\lambda_{max}(P)$ [20, Example 9.1]. With gains $K_2 > 0$ and $K_1 = 2\sqrt{K_2} > 0$ the origin of the unperturbed system (5) is exponentially stable [7, Lemma 2]. By [20, Lemma 9.2] the perturbed system will follow (24) and be ultimately bounded by (25). □

This theorem shows that the ultimate bound of the perturbed system (21) is proportional to δ, indicating that a small perturbation will not result in large steady-state errors. If the errors are sufficiently small then cooperating vehicles converge to a circular configuration under control (10).

Proposition 1. *Let* $f_k(t) = \beta(t) \in \mathbb{R}$ *satisfy* $|\beta| < 1$. *Also, let* $\hat{r}_k$ *and* $\hat{f}_k$ *evolve according to (21) with* $K_2 > 0$, $K_1 = 2\sqrt{K_2}$ *and bounded perturbation* $(g_k(t)\max(K_1, K_2)) \leq \delta$. *The distance between solutions of model (3) with the control (10) and the set of a circular formations with radius* $|\omega_0|^{-1}$ *and direction determined by the sign of* ω_0 *is ultimately bounded with ultimate bound proportional to* δ.

Figure 2 illustrates Proposition 1 for a uniform flowfield, $f = -0.5$, and position measurements perturbed by zero mean Gaussian noise with standard deviation σ truncated at $\delta = 3\sigma$. Figure 2(a) shows the stable circular formation of $k = 5$ particles. The red tracks indicate the noisy position measurements and the blue tracks show the actual particle position. With $K_2 = 2$ and $K_1 = 2\sqrt{K_2} = 2.83$, the constants in Lemma 1 become $c_1 = 0.204$, $c_2 = 1.298$, $c_3 = 1$ and $c_4 = 2.6$. Choosing $\epsilon = .99$ gives ultimate bound $b = 2.83$. A large ϵ value increases the bounding exponential but decreases the overall bound b. Figure 2(b) show the evolving errors for particle $k = 3$ as well as their bounding exponential functions and ultimate bound. The position error $e_{1,k} = \hat{r}_k - r_k$ with $\|e_{1,k}(t_0)\| = 3.2875$ is bounded by

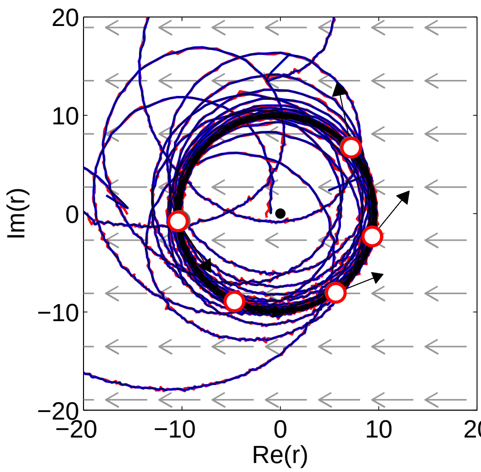

(a) $t = (0, 250)$ s.

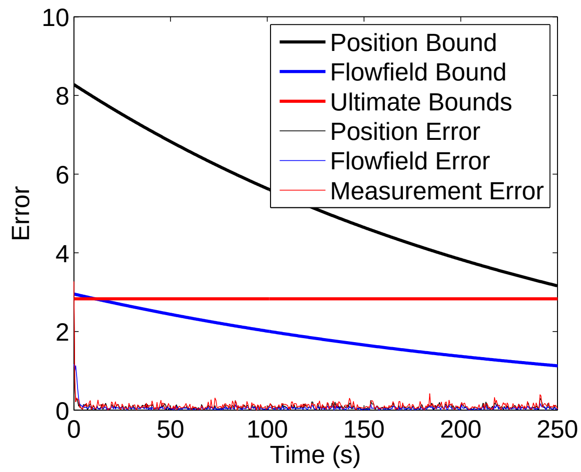

(b) $t = (0, 250)$ s.

Figure 2. Stabilization to a circular formation in an unknown uniform flowfield with noisy position measurements.

$24.1586e^{-0.0051t}$ (black lines). And the flowfield error $e_{2,k} = \hat{f}_k - f_k$ with $\|e_{2,k}(t_0)\| = 1.1726$ is bounded by $2.518e^{-0.0051t}$ (blue lines). Both errors are ultimately bounded by $b = 2.83$ (red line).

IV. Multi-Vehicle Flowfield Estimation and Control

This section describes two different methods for estimating a spatially varying, time-invariant flowfield and using that estimate in a motion coordination algorithm. Section IV.A implements a centralized information filter and Section IV.B a decentralized information-consensus filter for use when inter-vehicle communication is limited. Both approaches assume that each particle can measure the local flowfield at its current position. However, in Section IV.C we relax this assumption and instead use only noisy position measurements to estimate a local flowfield and subsequently, reconstruct the global flowfield.

The flowfield is approximated by a set of basis vectors as given by (11). The basis vectors are assumed to be known and the flowfield coefficients are estimated using the information filter described in Section II.B. The flowfield estimate $\hat{f}$ given by the information filter is used in control (10) to stabilize vehicles to a circular formation.

A. Centralized Flowfield Estimation Using an Information Filter

A centralized information filter is used when all-to-all communication is available among the cooperating vehicles. Figure 3(a) illustrates the architecture design. Each vehicle individually measures the local flowfield at its position, r_k. Equations (15) and (16) are used to

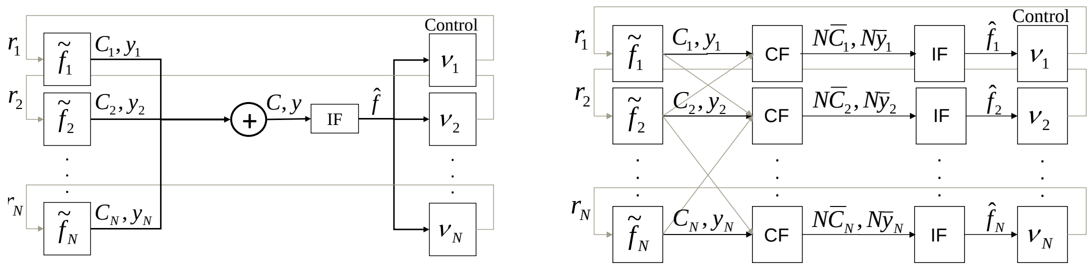

(a) Centralized information filter estimation with decentralized vehicle control.

(b) Decentralized information-consensus filter estimation and vehicle control.

Figure 3. Architecture comparison of the centralized information filter and decentralized information-consensus filter for flowfield estimation and multi-vehicle control.

obtain C_k and y_k. A centralized information filter sums C_k and $\boldsymbol{y}_k$ for all k and computes a single flowfield estimate, $\hat{f}$. The flowfield $\hat{f}$ and its directional derivative are fed into a decentralized controller for each particle, steering it to a circular formation. At the next time step this process is repeated and the global flowfield estimate is improved with the additional measurements. Table 1 provides this algorithm which simultaneously estimates the flowfield and uses that estimate in a multi-vehicle control.

For the following analysis we use the continuous form of the Kalman filter. The flowfield coefficients are constant, $\dot{\boldsymbol{a}} = 0$, and the flowfield measurement is given by (12). With a Kalman filter the estimated coefficients evolve according to

$$\dot{\hat{\boldsymbol{a}}}_k = K(\tilde{f}_k - \hat{f}_k) = K(\boldsymbol{\psi}_k^T \boldsymbol{a}_k + v_k - \boldsymbol{\psi}_k^T \hat{\boldsymbol{a}}_k), \tag{26}$$

where K is the Kalman filter gain matrix. Let the coefficient error for particle k be $\boldsymbol{e}_{3,k} = \hat{\boldsymbol{a}}_k - \boldsymbol{a}$. We have the following coefficient error dynamics

$$\begin{aligned} \dot{\boldsymbol{e}}_{3,k} &= \dot{\hat{\boldsymbol{a}}}_k - \dot{\boldsymbol{a}} = K(\tilde{f}_k - \hat{f}_k) && (27) \\ &= -K\boldsymbol{\psi}_k^T \boldsymbol{e}_{3,k} + K v_k && (28) \end{aligned}$$

Use (20) and (12) to obtain the dynamics for the velocity error

$$\begin{aligned} \dot{e}_{1,k} = \dot{\hat{r}}_k - \dot{r}_k &= (\hat{f}_k - f_k) - K_1(\hat{r}_k + g_k(t) - r_k) && (29) \\ &= (\boldsymbol{\psi}_k^T \hat{\boldsymbol{a}}_k - \boldsymbol{\psi}_k^T \boldsymbol{a}_k) - K_1(\hat{r}_k - r_k) - K_1 g_k(t) && (30) \\ &= \boldsymbol{\psi}_k^T \boldsymbol{e}_{3,k} - K_1 e_{1,k} - K_1 g_k(t) && (31) \end{aligned}$$

Table 1. Centralized Information Filter Cooperative Control Algorithm

Input: Basis vector $\boldsymbol{\psi}$, sensor variances R_k, and circle formation radius $|\omega_0|^{-1}$.
For each time step i; particle k, $k = 1, \ldots, N$:

1: Measures its position r_k exactly and flowfield $\tilde{f}_k$ with noise.

2: Evaluates the basis vectors at position r_k: $\boldsymbol{\psi}(r_k) = \boldsymbol{\psi}_k = [\psi_1(r_k), \psi_2(r_k), ..., \psi_l(r_k)]^T$.

3: Computes the information matrix C_k and information measurement $\boldsymbol{y}_k$ using equations (15) and (16).

4: Shares its information matrix and measurement vector with all other particles and computes C and $\boldsymbol{y}$ using C_k and $\boldsymbol{y}_k$, $k = 1, \ldots, N$.

5: Calculates the measurement updates (14) using the prior information covariance $I^-(t)$ and state $\hat{\boldsymbol{i}}^-(t)$ along with C and $\boldsymbol{y}$ calculated in step 4.

6: Finds the estimated flowfield coefficients $\hat{\boldsymbol{a}} = I^{-1}\hat{\boldsymbol{i}}$.

7: Computes the estimated flowfield $\hat{f} = \boldsymbol{\psi}_k\hat{\boldsymbol{a}}$.

8: Computes control ν_k (equation (10)) using the estimated flowfield $\hat{f}$.

9: Steers using turn-rate control $u_k = u_k(\nu_k)$, which is computed with the estimated flowfield $\hat{f}$ and directional derivative $\dot{\hat{f}}_k = (\partial \hat{f}_k / \partial r_k)\, \dot{r}_k$.

In matrix form the estimator-error dynamics are

$$\begin{bmatrix} \dot{e}_{1,k} \\ \dot{\boldsymbol{e}}_{3,k} \end{bmatrix} = \underbrace{\begin{bmatrix} -K_1 & \boldsymbol{\psi}_k^T \\ 0 & -K\boldsymbol{\psi}_k^T \end{bmatrix}}_{\triangleq A} \begin{bmatrix} e_{1,k} \\ \boldsymbol{e}_{3,k} \end{bmatrix} + \begin{bmatrix} -K_1 g_k(t) \\ K v_k \end{bmatrix}. \tag{32}$$

Under a noise-free system the error-dynamics reduce to

$$\begin{bmatrix} \dot{e}_{1,k} \\ \dot{\boldsymbol{e}}_{3,k} \end{bmatrix} = \underbrace{\begin{bmatrix} -K_1 & \boldsymbol{\psi}_k^T \\ 0 & -K\boldsymbol{\psi}_k^T \end{bmatrix}}_{\triangleq A} \begin{bmatrix} e_{1,k} \\ \boldsymbol{e}_{3,k} \end{bmatrix}. \tag{33}$$

Lemma 2. *Choosing gains $K_1 > 0$ and $K\boldsymbol{\psi}_k$ to be positive definite the error dynamics (33) exponentially stabilizes the origin $e_{1,k} = 0$ and $\boldsymbol{e}_{3,k} = \boldsymbol{0}\,\forall\, k$.*

Proof. The eigenvalues of the triangular matrix A are $\lambda_1 = -K_1$ and $\lambda_n = eig(-K\boldsymbol{\psi}_k)$, where $n = 1, \ldots, l$. Given that $K\boldsymbol{\psi}_k$ is positive definite $\lambda_n < 0$ for all n. Choosing $K_1 > 0$ results in $\lambda_1 < 0$. □

The following is a result of Lemma 2.

Lemma 3. *The matrix A defined in (33) is negative definite and the quadratic form*

$$Q_k(A) = \begin{bmatrix} e_{1,k} & \boldsymbol{e}_{3,k}^T \end{bmatrix} \begin{bmatrix} -K_1 & \boldsymbol{\psi}_k^T \\ 0 & -K\boldsymbol{\psi}_k^T \end{bmatrix} \begin{bmatrix} e_{1,k} \\ \boldsymbol{e}_{3,k} \end{bmatrix} = -K_1 e_{1,k}^2 - e_{1,k}\boldsymbol{\psi}^T\boldsymbol{e}_{3,k} + \boldsymbol{e}_{3,k}^T K \boldsymbol{\psi}_k^T \boldsymbol{e}_{3,k} \leq 0 \tag{34}$$

is equal to zero only when $e_{1,k} = 0$ and $\boldsymbol{e}_{3,k} = \boldsymbol{0}$ for $k \in \{1, \ldots, N\}$.

Consider the candidate Lyapunov function

$$\hat{S}(\hat{\boldsymbol{r}}, \hat{\boldsymbol{\gamma}}) \triangleq \frac{1}{2}\langle \hat{\boldsymbol{c}}, P\hat{\boldsymbol{c}} \rangle + \frac{1}{2}\left(||\boldsymbol{e}_1||^2 + ||\boldsymbol{e}_3||^2\right), \tag{35}$$

where $\boldsymbol{e}_1 = [e_{1,1}, e_{1,2}, ..., e_{1,N}]^T$, $\boldsymbol{e}_3 = [\boldsymbol{e}_{3,1}, \boldsymbol{e}_{3,2}, ..., \boldsymbol{e}_{3,N}]^T$ represent the noise-free error dynamics of (33) and $\hat{\boldsymbol{c}}$ is the vector of center points defined by (6). $\hat{S}$ is equal to zero when $\hat{\boldsymbol{c}} = c_0\boldsymbol{1}$, $c_0 \in \mathbb{C}$, and all estimation errors are zero. The time derivative of $\hat{S}$ along solutions of (3) and (33) is

$$\begin{aligned} \dot{\hat{S}} &= \sum_{k=1}^{N} (\langle \dot{\hat{c}}_k, P_k\hat{\boldsymbol{c}} \rangle + \dot{e}_{1,k}e_{1,k} + \dot{\boldsymbol{e}}_{3,k}\boldsymbol{e}_{3,k}) \\ &= \sum_{k=1}^{N} \left[\langle e^{i\hat{\gamma}_k}, P_k\hat{\boldsymbol{c}} \rangle (\hat{s}_k - \omega_0^{-1}\nu_k) + \underbrace{e_{1,k}(-K_1 e_{1,k} + \psi_k^T \boldsymbol{e}_{3,k}) + \boldsymbol{e}_{3,k}^T(-K\psi_k^T \boldsymbol{e}_{3,k})}_{\triangleq Q_k(A)} \right]. \end{aligned} \tag{36}$$

Substituting (10) into (36) shows that the time-derivative of the potential $\hat{S}(\hat{\boldsymbol{r}}, \hat{\boldsymbol{\gamma}})$ satisfies

$$\dot{\hat{S}} = \sum_{k=1}^{N} \left(-K\langle P_k\hat{\boldsymbol{c}}, e^{i\hat{\gamma}_k}\rangle^2 + Q_k(A)\right) \leq 0. \tag{37}$$

Using the invariance principle, all of the solutions of (2) with controller (10) converge to the largest invariant set where

$$-K\langle P_k\hat{\boldsymbol{c}}, e^{i\hat{\gamma}_k}\rangle^2 + Q_k(A) = 0, \ \forall\, k. \tag{38}$$

By Lemma 3 this is satisfied when $\langle P_k\hat{\boldsymbol{c}}, e^{i\hat{\gamma}_k}\rangle = 0$ and $Q_k(A) = 0$ independently. $Q_k(A) = 0$ implies that estimated values $\hat{r}_k$ and $\hat{\boldsymbol{a}}_k$ equal the measured values, r_k and $\boldsymbol{a}$. Values $\hat{\gamma}_k$, f_k and $\hat{s}_k$ are functions of $\hat{\boldsymbol{a}}_k$ and θ_k. This implies that $\hat{\gamma}_k$, f_k and $\hat{s}_k$ approach their measured values and, by (6), $\hat{c}_k$ converges to c_k. The condition, $\langle P_k\hat{\boldsymbol{c}}, e^{i\hat{\gamma}_k}\rangle = 0$ is satisfied for all k only when $P_k\hat{\boldsymbol{c}}$ is constant and equal to zero. Since the null space of P is spanned by $\boldsymbol{1}$ this implies $\hat{c}_k = \hat{c}_j$ for all k, j. In this set, control (10) evaluates to $\nu_k = \omega_0\hat{s}_k$ and $\dot{\hat{c}}_k = 0$, which

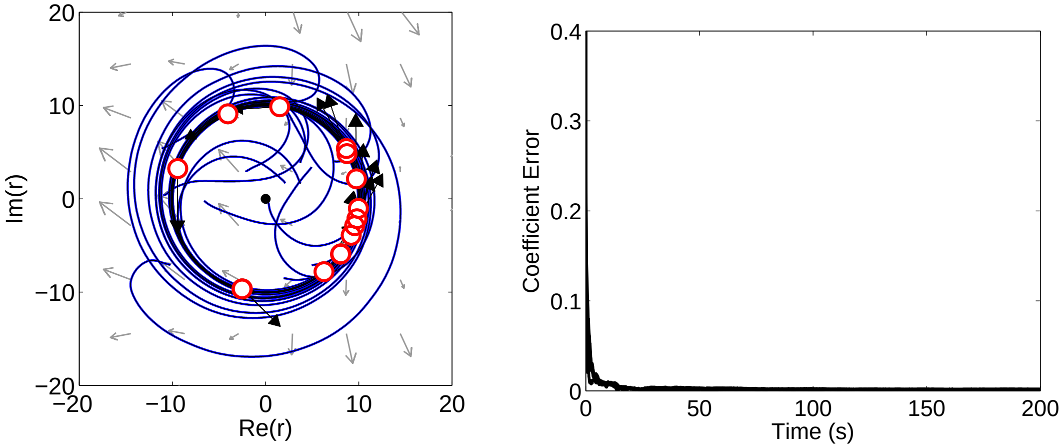

(a) $t = (0, 200)$ s.

(b) Flowfield coefficient error for particle $k = 15$.

Figure 4. This figure shows stabilization to a circular formation with an unknown, spatially varying flowfield estimated using a centralized information filter.

implies that each particle converges to circular motion around the same fixed center. For the noisy system (32) we can apply Lemma 1 to find ultimate bounds for the error.

Proposition 2. *Let $f_k = \sum_{n=1}^{l} a_n \psi_n(r_k)$ be a spatially-varying, time-invariant flowfield where $\psi_n(r_k)$ are known basis vectors, but the $\boldsymbol{a}_n$ are unknown. Also, let $\hat{r}_k$ and $\hat{\boldsymbol{a}}$ evolve according to (4) and (26) with $K_1 > 0$ and $K\boldsymbol{\psi}_k^T$ positive definite. Choosing control (10) forces convergence of solutions of model (3) to the set of a circular formations with radius $|\omega_0|^{-1}$ and direction determined by the sign of ω_0.*

Numerical simulations used the centralized information filter described in Table 1 to estimate the coefficients for a nonuniform flowfield. Figure 4 illustrates the results. The flowfield is modeled using a series of sines and cosines, $f_k = a_1 \sin(\mathrm{Re}(r_k)) + a_2 \cos(\mathrm{Im}(r_k)) + a_3 \sin(2\mathrm{Re}(r_k))i + a_4 \cos(2\mathrm{Im}(r_k))i$ with coefficients $a_1 = 0.5$, $a_2 = 0.5$, $a_3 = 0.5$, and $a_4 = 0.5$. The stabilized formation of $N = 15$ particles is shown in Figure 4(a) with a simulation time of $t = 200$ seconds. The tracks indicate that the particles have a short transient time when converging to the final formation. Figure 4(b) shows the error magnitude between the estimated and actual coefficients, $\hat{\boldsymbol{a}}_k - \boldsymbol{a}$ for $k = 15$. Despite being fed noisy flowfield measurements, the coefficient error converges to zero quickly.

B. Consensus-Based Flowfield Estimation Using Flow Measurements

In this section we use an information-consensus filter to estimate a spatially varying, time-invariant flowfield. Each particle uses the PI consensus filter introduced in Section II.B to calculate $\bar{C}_k$ the approximate average of matrix (15) and $\bar{\boldsymbol{y}}_k$ the approximate average of measurement vector (16). $\bar{C}_k$ and $\bar{\boldsymbol{y}}_k$ are multiplied by the number of particles N to

Table 2. Decentralized Information-Consensus Filter Cooperative Control Algorithm

Input: Basis vector $\boldsymbol{\psi}$, sensor variances R_k, circle formation radius $|\omega_0|^{-1}$, and communication topology.

For each particle k, where $k = 1, \ldots, N$, at each time step t:

1: Measure the exact position r_k and flowfield $\tilde{f}_k$ with noise.

2: Evaluate the basis vectors at position r_k: $\boldsymbol{\psi}_k = [\psi_1(r_k), \psi_2(r_k), ..., \psi_l(r_k)]^T$.

3: For $n = 1, \ldots, p$, where p is the number of consensus filter iterations, repeat: Use the consensus filter to estimate the components of C and $\boldsymbol{y}$.

4: Update the estimated coefficients $\hat{\boldsymbol{a}}_k$ using the information filter.

5: Compute control ν_k (equation (10)) using the flowfield $\hat{f}_k$.

6: Steer the particle using turn-rate control u_k, which is computed using the estimated flowfield $\hat{f}_k$ and estimated directional derivative $\dot{\hat{f}}_k = (\partial \hat{f}_k / \partial r_k)\, \dot{r}_k$.

approximate C and $\boldsymbol{y}$, which are used in distributed information filters to generate individual estimates of the flowfield coefficients. The estimated coefficients are fed into a control law that drives each particle to a circular formation. This process is depicted in Figure 3(b). To ensure faster convergence multiple consensus updates are performed for every steering control command. On a vehicle, the information-consensus filter would run as a separate process completing many consensus iterations between measurement update steps. Table 2 shows the iterative process each particle follows.

Numerical simulations are implemented using the information-consensus filter to generate individual estimates of the flowfield $\hat{f}_k$. The estimates were used in control (10) to stabilize a circular formation of $N = 15$ particles. The simulation results are depicted in Figure 5. Figure 5(a) shows the $N = 15$ particles converging to a circle over 250 seconds. The flowfield is modeled using $f_k = a_1 \sin(\mathrm{Re}(r_k)) + a_2 \cos(\mathrm{Im}(r_k)) + a_3 \sin(2\mathrm{Re}(r_k))i + a_4 \cos(2\mathrm{Im}(r_k))i$ with $a_1 = 0.5$, $a_2 = 0.5$, $a_3 = 0.5$, and $a_4 = 0.5$. The particles have a limited communication topology, communicating with only four neighbors, such that particle k receives communication directly from particles $k-2$, $k-1$, $k+1$ and $k+2$. It is assumed that the particle connection forms a ring so that neighbor $k-1$ for particle 1 is particle N. We set $K_I = 0.05$, $K_P = 0.5$, $\phi = .01$, and assumed sensor variance $R_k = .01$. Figure 5(b) shows how for the coefficient errors, $\hat{\boldsymbol{a}}_k - \boldsymbol{a}$ where $k = 15$, the error converges to zero. The error values for the consensus filter take longer to converge than the centralized implementation (Figure 4(b)) due to the imperfect estimates of C and $\boldsymbol{y}$. This increases the transient time for the particles to stabilize to a circular formation.

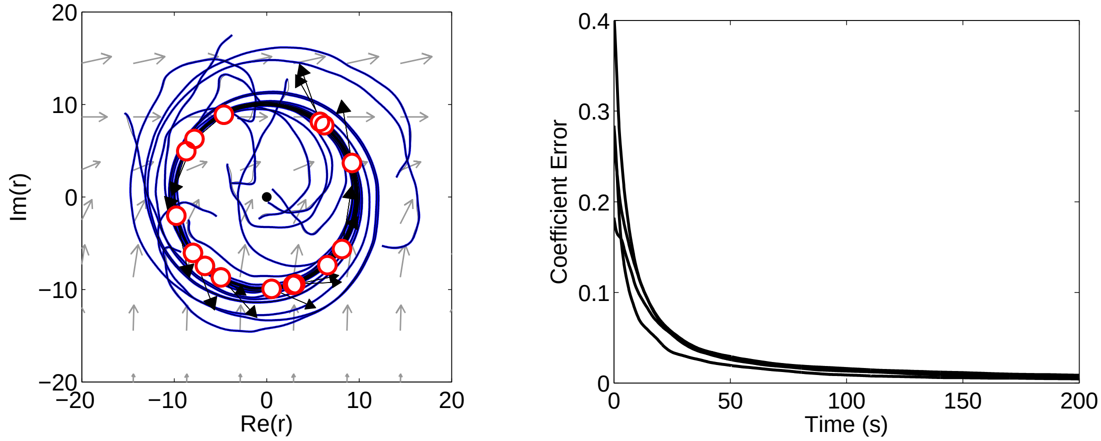

(a) $t = (0, 250)$ s.

(b) Flowfield coefficient errors for particle $k = 15$.

Figure 5. Stabilization to a circular formation in an unknown spatially varying flowfield when a decentralized information-consensus filter is used to estimate the flow.

C. Consensus Based Flowfield Estimation Using Noisy Position Measurements

In this section we relax the assumption that each particle measures the local flowfield. Instead the flowfield is estimated using noisy position measurements. Let $m_k(t)$ be the discrete-time measured position difference at time t,

$$m_k(t) = r_k(t) - r_k(t - \Delta t) + v_k(t). \tag{39}$$

where $v_k(t)$ is Gaussian, zero-mean noise and

$$\dot{\boldsymbol{r}}_k = \lim_{\Delta t \to \infty}(r_k(t) - r_k(t - \Delta t)). \tag{40}$$

For a sufficiently small Δt, θ_k is constant. Substituting (1) into (39) yields

$$\begin{aligned} m_k(t) &\approx [e^{i\theta_k(t)} + f_k(t)]\Delta t + v_k(t) \\ m_k(t) &\approx [e^{i\theta_k(t)} + \tilde{f}_k(t) - v_k(t)]\Delta t + v_k(t) \end{aligned} \tag{41}$$

The local flowfield measurement can be approximated by

$$\hat{\tilde{f}}_k(t) \approx \tfrac{m(t)}{\Delta t} - e^{i\theta_k} + (\Delta t - 1)\tfrac{v_k(t)}{\Delta t}. \tag{42}$$

$\hat{\tilde{f}}_k(t)$ is used in place of local measurements in the centralized information filter of Section IV.A or consensus filter of Section IV.B to estimate the global flowfield. In order to estimate a local flowfield we need to know both the orientation of the velocity relative to the flow θ_k and the speed relative to the flow. The latter value equals one under our unit speed

Table 3. Decentralized Consensus Filter Cooperative Control Algorithm

Input: Basis vector $\boldsymbol{\psi}$, sensor variances R_k, circle formation radius $|\omega_0|^{-1}$, and communication topology.

For each particle k, where $k = 1, \ldots, N$, at each time step t:

1: Measure the noisy position $\tilde{r}_k$.

2: Use the difference between the previous and current position measurement to to estimate the local flowfield measurement (42).

3: Evaluate the basis vectors at the measured position $\tilde{r}_k$: $\boldsymbol{\psi}(\tilde{r}_k) \triangleq \tilde{\boldsymbol{\psi}}_k = [\psi_1(\tilde{r}_k), \psi_2(\tilde{r}_k), ..., \psi_l(\tilde{r}_k)]^T$.

4: For $n = 1, \ldots, p$, where p is the number of consensus filter iterations, repeat: Use the consensus filter to estimate the components of C and $\boldsymbol{y}$.

5: Update the estimated coefficients $\hat{\boldsymbol{a}}_k$ using the information filter.

6: Compute control ν_k (equation (10)) using the flowfield $\hat{f}_k$.

7: Steer the particle using turn-rate control u_k, which is computed using the estimated flowfield $\hat{f}_k$ and estimated directional derivative $\dot{\hat{f}}_k = (\partial \hat{f}_k / \partial r_k)\, \dot{r}_k$.

particle model. The modified information-consensus filter algorithm which utilizes noisy position measurements to estimate the local flowfield is given in Table 3. Figure 6 shows the estimated local flowfield incorporated into the information-consensus filter architecture.

Figure 7 shows the convergence of $N = 15$ particles to a circular configuration. Each particle individually estimates the local flowfield using (42). The local flowfield estimate is used with an information-consensus filter (as described in Section IV.B) to estimate the coefficients for the flowfield. The global flowfield is modeled with a series of sin and cosine functions, $f_k = a_1 \sin(\mathrm{Re}(r_k)) + a_2 \cos(\mathrm{Im}(r_k)) + a_3 \sin(2\mathrm{Re}(r_k))i + a_4 \cos(2\mathrm{Im}(r_k))i$ with $a_1 = 0.5$, $a_2 = 0.5$, $a_3 = 0.5$, and $a_4 = 0.5$. Figure 7(b) shows the decrease in error between the estimated and actual flowfield coefficients, $\hat{\boldsymbol{a}}_k - \boldsymbol{a}$ for particle $k = 15$. Using noisy position measurements to (1) estimate the flowfield and (2) steer the particles increases the time it takes to converge to the circular formation.

V. Conclusion

This paper describes the design of decentralized control algorithms for autonomous vehicles that operate in the presence of unknown flowfields. For a uniform flowfield each vehicle individually estimates the flow using noisy position measurements. It was proven that this estimator is robust to perturbations. Spatially varying flowfields were estimated using a cen-

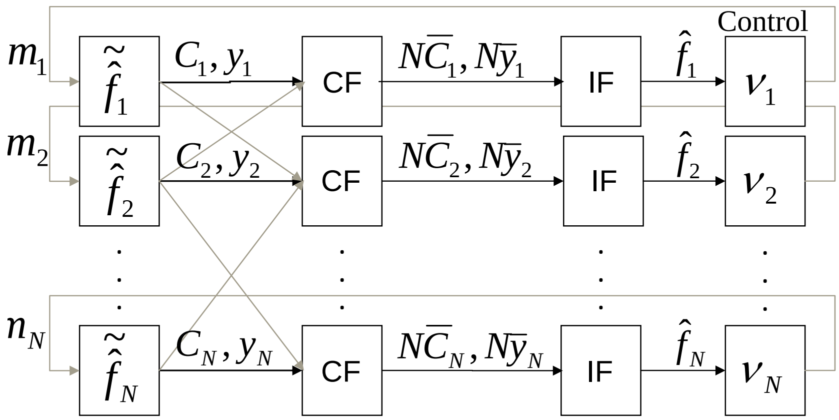

Figure 6. Information-consensus filter architecture when using noisy position measurements to estimate the flowfield.

tralized information filter and a decentralized information-consensus filter, the later being necessary when inter-vehicle communication is limited. The information filter reconstructed the flowfield and the consensus filter shared information between vehicles. Each vehicle used only its noisy position measurement to determine an approximate estimate of the local flowfield. The flowfield estimate was used to stabilize multiple vehicles to circular configurations. Simulations showed that the centralized information filter and the decentralized information-consensus filter both converged to the same result.

Acknowledgments

This material is based upon work supported by the National Science Foundation under Grant No. CMMI0928416 and the Office of Naval Research under Grant No. N00014-09-1-1058.

References

[1]Frew, E. W., Lawrence, D. A., and Morris, S., "Coordinated Standoff Tracking of Moving Targets Using Lyapunov Guidance Vector Fields," *J. Guidance, Control, and Dynamics*, Vol. 31, No. 2, 2008, pp. 290–306.

[2]Summers, T. H., Akella, M. R., and Mears, M. J., "Coordinated Standoff Tracking of Moving Targets: Control Laws and Information Architectures," *J. Guidance, Control, and Dynamics*, Vol. 32, No. 1, 2009, pp. 56–69.

[3]Sepulchre, R., Paley, D. A., and Leonard, N. E., "Stabilization of planar collective motion: All-to-all communication," *IEEE Trans. Automatic Control*, Vol. 52, No. 5, 2007, pp. 811–824.

[4]Sepulchre, R., Paley, D. A., and Leonard, N. E., "Stabilization of planar collective motion with limited communication," *IEEE Trans. Automatic Control*, Vol. 53, No. 3, 2008, pp. 706–719.

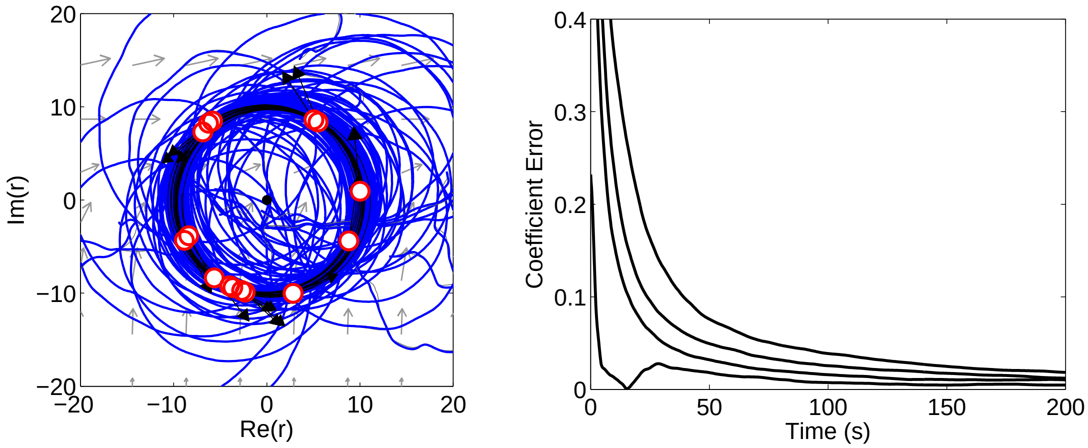

(a) $t = (0, 500)$ s.

(b) Flowfield coefficient errors for particle $k = 15$.

Figure 7. Stabilization to a circular formation in an unknown spatially varying flowfield with local and global flowfield estimation.

[5]Techy, L., Paley, D. A., and Woolsey, C. A., "UAV Coordination on Convex Curves in Wind: An Environmental Sampling Application," *Journal of Guidance, Control, and Dynamics*, Vol. 33, 2010, pp. 1946.

[6]Burger, M. and Pettersen, K. Y., "Curved Trajectory Tracking for Surface Vessel Formations," *49th IEEE Conference on Decision and Control*, Dec. 2010, pp. 7159–7165.

[7]Peterson, C. and Paley, D. A., "Multi-vehicle Coordination in an Estimated Time-Varying Flowfield," *Journal of Guidance, Control, and Dynamics*, Vol. 34, No. 1, 2011, pp. 177–191.

[8]Lynch, K. M., Schwartz, I. B., Yang, P., and Freeman, R. A., "Decentralized environmental modeling by mobile sensor networks," *IEEE Transactions on Robotics*, Vol. 24, No. 3, 2008, pp. 710–724.

[9]Olfati-Saber, R., Fax, J. A., and Murray, R. M., "Consensus and cooperation in networked multi-agent systems," *Proceedings of the IEEE*, Vol. 95, No. 1, 2007, pp. 215–233.

[10]Ren, W., Beard, R. W., and Atkins, E. M., "A survey of consensus problems in multi-agent coordination," *Proceedings of the American Control Conference*, 2005, pp. 1859–1864.

[11]Casbeer, D. W., *Decentralized Estimation Using Information Consensus Filters with a Multi-Static UAV Radar Tracking System*, Ph.D. thesis, Brigham Young University, 2009.

[12]Casbeer, D. W. and Beard, R., "Distributed Information Filtering using Consensus Filters," *Proceedings of the American Control Conference, 2009*, No. 1, pp. 1882–1887.

[13]Olfati-Saber, R., "Distributed tracking for mobile sensor networks with information-driven mobility," *Proceedings of the American Control Conference, 2007*, pp. 4606–4612.

[14]Olfati-Saber, R. and Shamma, J., "Consensus Filters for Sensor Networks and Distributed Sensor Fusion," *Proceedings of the 44th IEEE Conference on Decision and Control*, 2005, pp. 6698–6703.

[15]Olfati-Saber, R., "Distributed Kalman Filter with Embedded Consensus Filters," *Proceedings of the 44th IEEE Conference on Decision and Control*, 2005, pp. 8179–8184.

[16]Olfati-Saber, R., "Kalman-Consensus Filter : Optimality, stability, and performance," *Proceedings of the 48th IEEE Conference on Decision and Control held jointly with 28th Chinese Control Conference*, Dec. 2009, pp. 7036–7042.

[17]Paley, D. A. and Peterson, C., "Stabilization of collective motion in a time-invariant flowfield," *Journal of Guidance, Control, and Dynamics*, Vol. 32, No. 3, 2009.

[18]Simon, D., *Optimal State Estimation: Kalman, H infinity and nonlinear approaches*, John Wiley & Sons, Inc., New Jersey, 2006.

[19]Fax, J. A. and Murray, R. M., "Information flow and cooperative control of vehicle formations," *IEEE Transactions on Automatic Control*, Vol. 49, No. 9, 2004, pp. 1465–1476.

[20]Khalil, H. K., "Advanced Stability Analysis," *Nonlinear Systems*, chap. 9, Prentice Hall, 3rd ed., 2002, pp. 303–338.